Advances in Aerodynamics

RESEARCH Open Access

Visual analytics of combustion on time-varying turbulent-flow

Xiaoyang Han[1,2], Yifei An[1,2], Guihua Shan[1,2*], Jun Liu[1] and Bo Yang[1]

*Correspondence: sgh@sccas.cn
[1]Computer Network Information Center, Chinese Academy of Sciences, Beijing, China
[2]University of Chinese Academy of Sciences, Beijing, China

Abstract

Visualization is crucial for analyzing the turbulent combustion simulation. Time-varying data allows us to investigate the evolution process of the turbulent flow field. To study the combustion effects, we calculated the enstrophy of the flow field since high enstrophy region can display valuable features, and extract components based on these features. We isolated large components to track their behaviors and characterized them using volume and spatial locations, which helps scientists to explore the dynamics and temporal changes of intense events individually. We analyzed the components' structures and visualized them in contouring and statistical charts.

Keywords: Turbulent combustion, Supersonic jet, Turbulent-flow visualization

1 Introduction

The development of scramjet brings urgent need for visualizing time-varying turbulent combustion flow. Interaction between combustion and turbulence can be complicated. Turbulence is sufficiently intense, and filamentary structures can appear. On the other hand, turbulence itself is a complex phenomenon in fluid mechanics simulation involving time and space scales [1]. Therefore, it is critical to understand turbulent flow and its behavior.

However, how to efficiently display turbulent combustion and its inherent characteristics has always been an important issue. Visualization and analysis of turbulent combustion provide a powerful way to understand it. Thanks to the great advancement of super computing and numerical theories, computational fluid dynamics (CFD) methods, including direct numerical simulation (DNS), large eddy simulation (LES), Reynolds-averaged Navier-Stokes equations (RANS), have become a promising and necessary method to understand the intrinsic characteristics of the turbulent flow [2]. Many scientists have focused on visualizing turbulent flow. For example, Hin et al. [3] visualized turbulent flow in 3D using particle visualization. Mynett et al. [4] used particle tracing technique presented in turbulent flow to combine both mean and fluctuating velocity vectors. Johnson et al. [5] proposed an interactive visualization system for the interactive exploration of large-scale datasets. Visualization provides an opportunity to explore the strong structure and evolutionary dynamics. Understanding these structures provides an

important way to fully understand turbulence and other detailed engineering applications [6]. The ultimate goal is to understand and control the mechanism of turbulent jets [7].

To describe and understand the characteristics of the time-varying turbulent flow structure, we have developed a method for visualization and analysis of turbulent combustion simulations, and proved the analysis relevance through related theories of information theory. For the turbulent combustion process, we visualized the time series volume, and analyzed the changes of enstrophy during different periods of combustion. Our main contributions are summarized as follows.

- Apply a novel pipeline to extract intense features in turbulent flow and visualize them
- Analyze a large turbulent combustion simulation, and discuss the evolution of structures and statistics of turbulent fluctuations
- Analyze the visualization of enstrophy through information entropy and mutual information

2 Related work

We reviewed the topics related to our work in turbulent flow and scientific visualization.

2.1 Turbulent flow

The application of turbulent flow has been widely discussed in the field of engineering. The mechanism of interaction between combustion and turbulence is a trending topic in recent years. Luo et al. [8] developed a fully compressible solver for direct numerical simulation of supersonic combustion and applied it to investigate a three-dimensional spatially-developing supersonic turbulent jet flame. Papamoschou et al. [9] focused on growth rate and turbulent structure of the compressible, plane shear layer, and they defined a compressibility-effect parameter where convective Mach number is used. Li et al. [10] studied the influence of turbulence intensity on flame local structural and local propagation characteristics. Wacks et al. [11] investigated the distribution of flow topologies of turbulent combustion. Rao et al. [12, 13] conducted experiments on a reference conical nozzle of Mach number 1.8 to study far-field flow structure of supersonic free jets from complex nozzles. Bogey et al. [14] applied LES on researching the influences of different Reynolds numbers on jet self-similarity. Zhou et al. [15] visualized the flame front structures in swirl-stabilized lean premixed methane/air flames. The results showed that the investigated flames exhibit various flame front structures distinctly in space. Slessor et al. [16] proposed a new shear-layer growth-rate compressibility-scaling parameter as an alternative to the total convective Mach number. And Boersma et al. [17] considered the direct numerical simulation (DNS) of a spatially developing free round jet at low Reynolds numbers. However, there are few papers visualizing the influences of the combustion on turbulence characteristics and evolution.

2.2 Flow visualization

Effective analysis of vector fields plays a fundamental role in many scientific disciplines, such as aerodynamics, climate, and computational fluid dynamics. Flow visualization has been a significant topic in scientific visualization for three decades. Integration-based [18] methods extract geometric objects such as streamlines from the data for visualization. Associated methods focus on identifying streamlines with unique geometric features, as

the shape of streamlines is often related to some underlying property of the field. Han et al. [19] applied a recurrent generative model for generating temporal super-resolution of a volume sequence data. Then Guo et al. [20] extended the work to spaital super-resolution, where they used the generative adversarial network to generate high-resolution time-varying volumes. Chaudhuri et al. [21] introduced box counting ratio to quantify the geometric complexity of streamlines. Recently, Lu et al. [22] used the distribution of feature measures over a streamline to measure the similarity between streamlines. He et al. [23] applied deep learning on the visualization images from the simulation and viewing parameters to support parameter exploration. To our knowledge, there is no relevant work on performing spatial-temporal super-resolution on vector field to improve the data reduction rate and post-hoc visualization results, which is our focus. Recently, many techniques focused on the special meaning of the visualization. Feature-based flow visualization brings the visualization to a higher level of abstraction by extracting and showing only those meaningful parts to researchers. Wilde et al. [24] presented a formal approach to the visual analysis of recirculation in flows by introducing recirculation surfaces for 3D unsteady flow fields. Tao et al. [25] introduced semantic flow graph (SFG), a novel graph representation and interaction framework that enables users to explore the relationships among key objects of a 3D flow field.

3 Background

Turbulent flow is the most common phenomenon of fluid motion and physical simulation. Understanding turbulence is critical in many applications such as aerodynamics, combustion processes and climate. Turbulent flow can be characterized by nonlinear stochastic fluctuations. DNS can compute instantaneous velocity and pressure fields according to the Navier Stokes equations. The conservative three-dimensional compressible Navier-Stokes equations together with the conservation equations of species are given as:

$$\begin{aligned}
\frac{\partial \rho}{\partial t} + \frac{\partial (\rho u_i)}{\partial x_i} &= 0 \\
\frac{\partial (\rho u_i)}{\partial t} + \frac{\partial \left(\rho u_i u_j\right)}{\partial x_j} &= 0 \\
\frac{\partial E}{\partial t} + \frac{\partial \left[(E+P)u_j\right]}{\partial x_j} &= \frac{\partial \left[u_i \tau_{ij} + q_j\right]}{\partial x_j} + Q_s \\
\frac{\partial \rho_k}{\partial t} + \frac{\partial (\rho_k u_i)}{\partial x_i} &= \frac{\partial}{\partial x_i}\left[\rho D_{km} \frac{\partial Y_k}{\partial x_i}\right] + \dot{\omega}_k
\end{aligned} \tag{1}$$

where ∂ is a partial derivative, ρ is the density of mixture, u_i is the fluid velocity, P is the static pressure, and ρ_k is the density of species k, which can be expressed as $\rho_k = \rho Y_k$. E and Q_s are the total energy per unit volume and heat release rate. $\dot{\omega}_k$ is the production rate of species k. D_{km} is the mixture diffusion coefficient of species k. τ_{ij} is the viscous stress tensor, and Y_k is the mass fraction of species k. In present simulations, standard forms of polynomial fits used by NASA chemical equilibrium code [26] are employed to calculate the thermodynamic properties. Numerical simulation of high Reynolds number turbulence is still a great challenge in high-performance computing since it demands speed and memory. The simulation we study is three dimensional spatially-developing supersonic round turbulent hydrogen jets, which contains chemical reaction.

To analyze the chemical reacting flows, our group develop a high order finite difference solver, OpenCFD-Comb, used for DNS cases. The inlet condition of the round jet flow is the same as [8, 27–29], where the volume of the supersonic jet consists of 85% hydrogen and 15% nitrogen, and the jet has a temperature of 305 K and a jet velocity of 900 m/s. The ambient air velocity is 20 m/s and the temperature is 1150 K. The jet exit diameter, denoted as D, is 1.44 mm. The Reynolds number based on the jet exit diameter and hydrogen jet velocity is 22000 and the jet Mach number is $Ma = \frac{U_j}{a_j} = 1.2$. Note, U_j is the hydrogen jet velocity and a_j is the sound velocity of jet exit. A large enough computation domain is designed in a Cartesian coordinate system as $0 \leq 15D, -7D \leq y \leq 7D, -7D \leq z \leq 7D$. The total structured nodes number is $670 \times 459 \times 459$, and the size of each cell is about $0.03 \times 0.04 \times 0.04$ mm^3. The dataset consists of 14 time steps.

4 Methods

In order to perform a visual analysis of combustion turbulence, we mainly calculated enstrophy, visualized the contour of the component, and quantified the properties of the component, and then performed a statistical analysis of the component. In addition, we also carried out tracking analysis for turbulence.

4.1 Enstrophy

The analysis of turbulent-flow mostly focuses on enstrophy, a quantity directly related to the kinetic energy that corresponds to dissipation effects in the fluid flow. Researchers seek to explore the shape and structure of dissipation around high-enstrophy areas. Given a vector field $u \in \Omega$, where Ω represents the entire combustion domain, enstrophy can be computed as:

$$\mathcal{E}(u) = \int_{\Omega} |\nabla \mathbf{u}|^2 dx \tag{2}$$

where $|\nabla \mathbf{u}|^2 = \sum_{i,j=1}^{n} \left|\partial_i u^j\right|^2$. In the case of incompressible flow, the enstrophy can be described as the integral of the square of the vorticity. Regions of high enstrophy require further study since they can demonstrate valuable features. We apply volume rendering visualization to isolate areas where enstrophy is higher than a fixed value, which is suggested by domain experts. In this work, we isolate areas with enstrophy greater than 10000. Since we are managing large-scale dataset, we look into how high-activity regions look like in space and how they evolve over time. Thus we also use contouring visualization technique to extract the components where the enstrophy value is greater than 30000 and to track their behaviors. We call the components extracted in this step as high enstrophy area and the rest as low enstrophy area. To this extent, we can count the number of components and calculate their attributes like centroid or number of cells.

4.2 Tracking features

Tracking features is not a new concept [30]. For example, eddy tracking has always been a hot topic in eddy visualization [31, 32]. For time-varying turbulent flow, we can also characterize the components and analyze their properties like volume and location. A connected component is a set of connected cells in space. For every time step, we calculated a distance matrix from one component to each other at the same step. Then we

recorded their properties and locations. We then computed the neighbors of all components for the next time step, and found the most similar component to themselves at every property as their next location. We have a threshold value to compute the neighbors of the components. It is based on the components distance matrix across all the time steps. We set it by their distance distribution.

4.3 Information entropy and mutual information

Information entropy is a statistical form of 2D/3D features that reflects the average amount of information in the image or volume. It can be calculated as follows, where P_i represents the frequency of occurrence of event i among m events of random variable X.

$$H(X) = -\sum_{i=1}^{m} P_i \log P_i \tag{3}$$

On the basis of information entropy, mutual information is a measure of the degree of interdependence between random variables. The calculation method of mutual information is as follows. $P(x)$ and $P(y)$ are marginal probability distributions. $P(x, y)$ is the joint probability distribution of random variables X and Y. It can be further simplified using information entropy. The simplified formula can directly explain the meaning of mutual information, that is, the amount of information reduced by the initial random variable X after knowing fact Y.

$$I(X;Y) = \sum_{y\in\gamma}\sum_{x\in\chi} P(x,y)\log\frac{P(x,y)}{P(x)P(y)} = H(X) - H(X|Y) \tag{4}$$

5 Visualization

To better understand the insight of the massive flow fields, we use enstrophy to extract attractive components and potential regions. By using properties of components to track their behavior across time, we visualized the volume of all the large components to show the trend of components' shapes and sizes with time-varying simulation. The mutual information visualization provides the correlation between combustion velocity field and the enstrophy of the combustion turbulence.

5.1 Enstrophy analysis

By visualizing the enstrophy at different value, we analyzed a large turbulent combustion simulation, and discussed the evolution of structures and statistics of turbulent fluctuations. As shown in Fig. 1, we visualized the components with high enstrophy over time (color highlight parts), and we can see that during the first time step, small components form up a circle at the front, then it dissipates and disappears in the following process. The high enstrophy part begins to aggregate in the middle region of the turbulent flow over time. The figures (outside the color highlight parts) also refer to components with low enstrophy value, where the components connect together and form a larger shape. For example, they have a complete circular ring in the head of the jet combustion. At the very beginning, the scattered components form a donut winding in the middle region, and then they move backward and amalgamate with posterior components. We can see that in the middle area, some small components grow larger and become one larger component. In the rear area, we can observe that there are some large flat structures at the beginning,

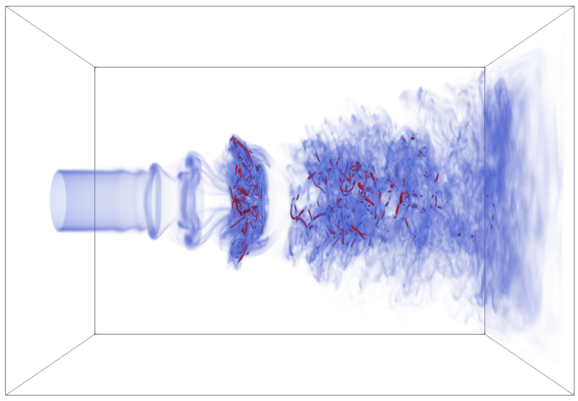

(a)

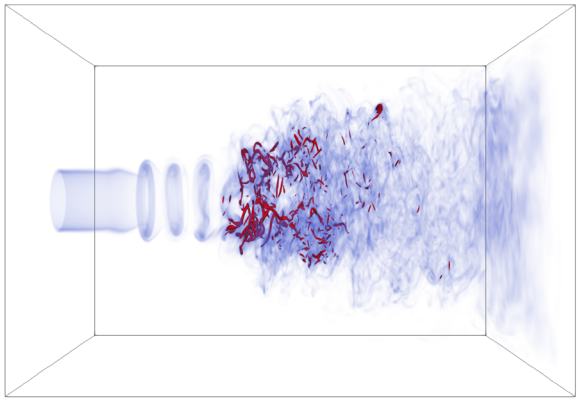

(b)

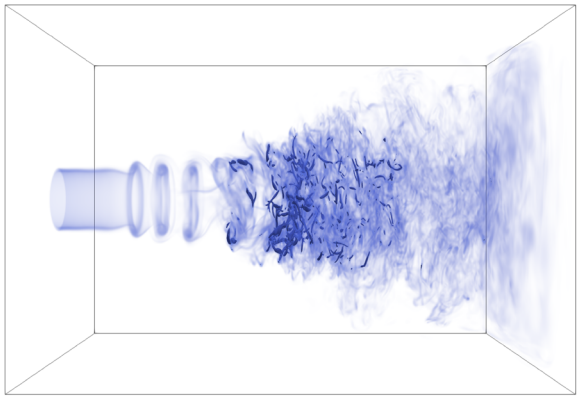

(c)

Fig. 1 Volume visualization of enstrophy and overtime for all the large components (parts of color highlight). Most components have a volume of 20 cells to 30 cells. **a** the start time step of the combustion simlulation. **b** the middle time step. **c** the end time step

but they disappear at the end time, and the components also move to the middle area and amalgamate into fusiform structure.

5.2 Components trace

Other than visualization of the contouring of the components, we wanted to quantify the property of the components. Thus, we calculated the volume of the components for high enstrophy value and low enstrophy value. Then we visualize them as frequency histogram.

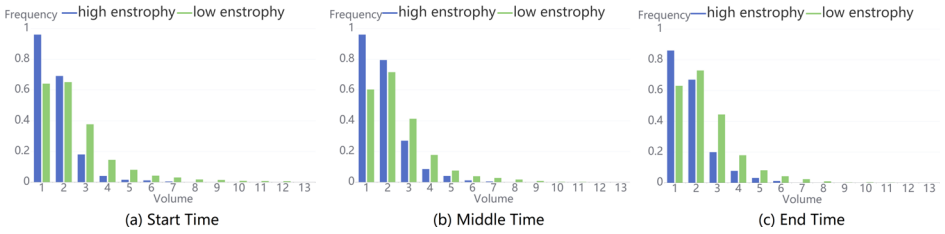

Fig. 2 The frequency histogram for the volume of the components at different levels of enstrophy value during different time of combustion. **a** Start time. **b** Middle time. **c** End time

As the volume distribution ranges of low and high enstrophy components are different, we define the total number of bins of the histogram to be 64, which is larger than the actual number. As we can see in Fig. 2, at all time, high enstrophy components tend to have smaller volume, since the distribution of volume at high enstrophy aggregates at low values. However, the volume of low enstrophy components is relatively large. The maximum volume of the high enstrophy components is about 7 cells, while the low enstrophy components can reach 13 cells.

At the start time of the combustion process, high enstrophy components tend to have smaller volume, and over time, the percentage of small volume components decreases. But for low enstrophy components, this kind of trend doesn't appear.

We also performed statistical analysis on the components. For example, in Fig. 3, we calculated the total volume, the max volume for the components at high enstrophy value and low enstrophy value over time separately. After visualization, we can see that the total volume of high and low enstrophy components tends to increase over time and then decrease at the end of the combustion. And the volume of low enstrophy components is larger than the high enstrophy components. For the max volume of the components, the low enstrophy components have smaller fluctuation range, but we can still observe that it first rises to a high level and then falls. For high enstrophy value, the trend is more obvious.

Then we isolated high enstrophy components and tracked them over time. The number of components is enormous, which makes it hard to isolate them from each other and classify the components. Thus, we filtered the components with a total volume below a fixed value. In this manner, we reduce the number of components and focus more on

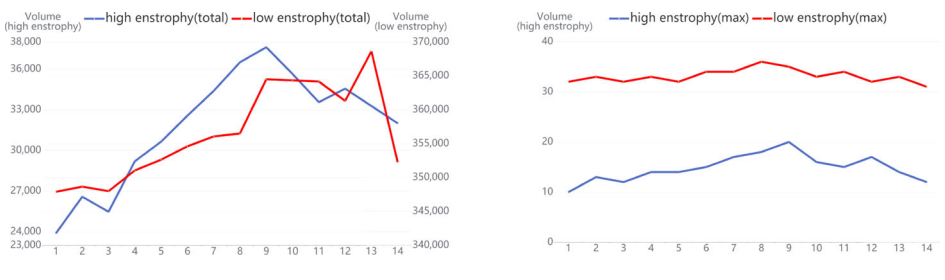

Fig. 3 The line plot for the volume of the components at different enstrophy value during different time of combustion. The left is the total volume of the components, and the right is the max volume of the components. The blue line indicates high enstrophy value, and the red line indicates low enstrophy value

the salient, connected structures, which makes it easier to track them. We determine a center coordinate of each component based on the coordinates of its boundary points. At every two adjacent time steps, we treat the two components whose center coordinates are closest to each other as the same component. For each component tracked, we set a distance range, and if there are no new components in the range at the next time step, the evolution of the component is considered finished.

To track the evolution of the component in the turbulent combustion process, we use the turbulence generated by the unstable spherical burst simulation process to track the high enstrophy components. Through the above component tracking method, we visualized the visualization results of the high components of the surface at several consecutive time steps when turbulence was generated, as shown in the figure. As shown in Fig. 4, yellow, blue, white, and red are the evolution of the high component of turbulence in 4 consecutive periods. It can be seen that it gradually decreases and dissipates in the process of outward diffusion. Among them, the ring structure of the high component of turbulence at the fourth time step (red) has begun to dissipate.

We then visualized the volume at every time step for each component. In Fig. 5, we can observe that the volume of components ranges from 17 cells to 35 cells, but mostly from 20 cells to 30 cells. The change in volume from time to time follows consistent trends over the whole time, which makes the track process more valid. We can see a global trend that the volume for most components increases initially and decreases afterwards. The volume reaches its peak at middle time of the simulation of combustion.

5.3 Mutual information

To further illustrate the effectiveness of our visual analysis system, we evaluate the results of visualization of enstrophy by calculating the mutual information between enstrophy and velocity field and performing normalization calculations. As shown in Fig. 6, the first

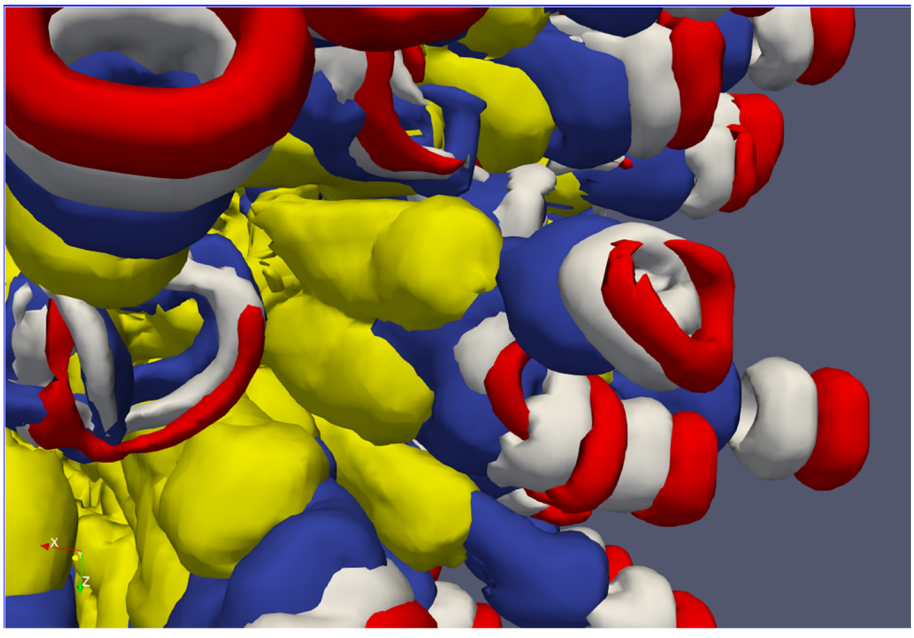

Fig. 4 Evolution of the high component of turbulence in 4 consecutive periods

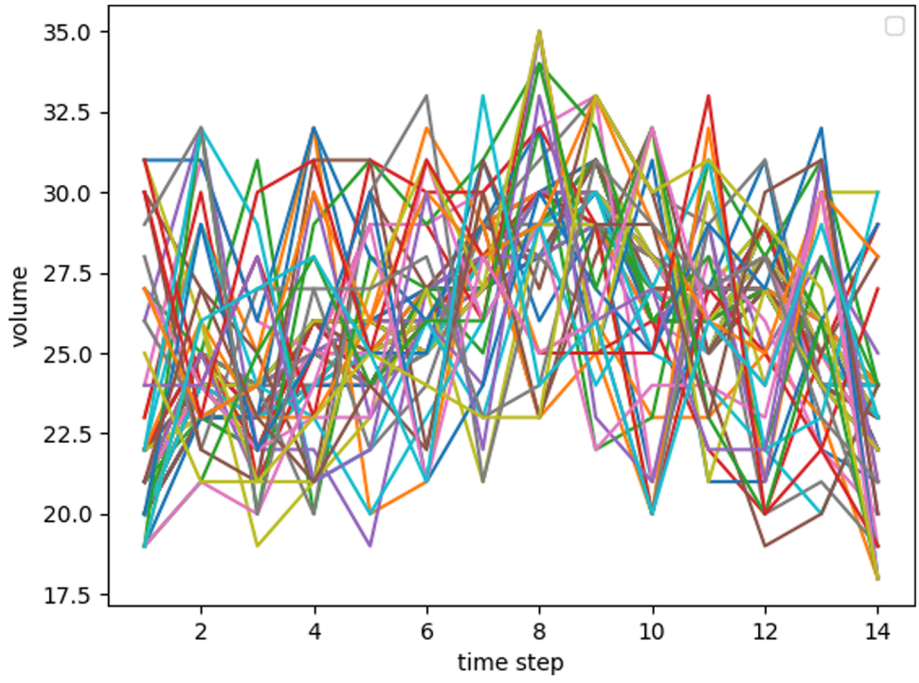

Fig. 5 Volume overtime for all the large components. Most components have a volume of 20 to 30

and second rows of the figure respectively visualize the distribution of the data velocity field and the corresponding enstrophy distribution. The value of mutual information is 0.999 throughout the simulation process. It can be seen that the enstrophy distribution and the velocity field distribution have some similarities in the visualization results. The calculation results of mutual information show that enstrophy and the combustion velocity field have a very high correlation, which can better deal with the analysis and visualization of combustion turbulence.

6 Conclusion

In this paper, we proposed a visualization pipeline for turbulent-flow of combustion, which provides a better understanding for the insight of the massive flow fields and allows user to better comprehend the physical processes of the jet combustion. Using enstrophy to extract components which may have intense behaviors allows us to find the potential region that may be worth paying attention to.

Through our system, experts used properties of components to track their behavior across time. They set a threshold value for tracking features based on their distance distribution and visualized the volume of all the large components. Experts found that in turbulent combustion, the volume of most components initially increases and then decreases, and the volume reaches its peak in the middle of the simulated combustion. In addition, the mutual information between the combustion velocity field and the enstrophy of the combustion turbulence performed a visual comparison and analysis. Through the analysis and comparison, experts obtained the following conclusions:

- The jet combustion will create many thin turbulent flow components. Some circular winding structures will appear at first, then break into pieces and disappear.

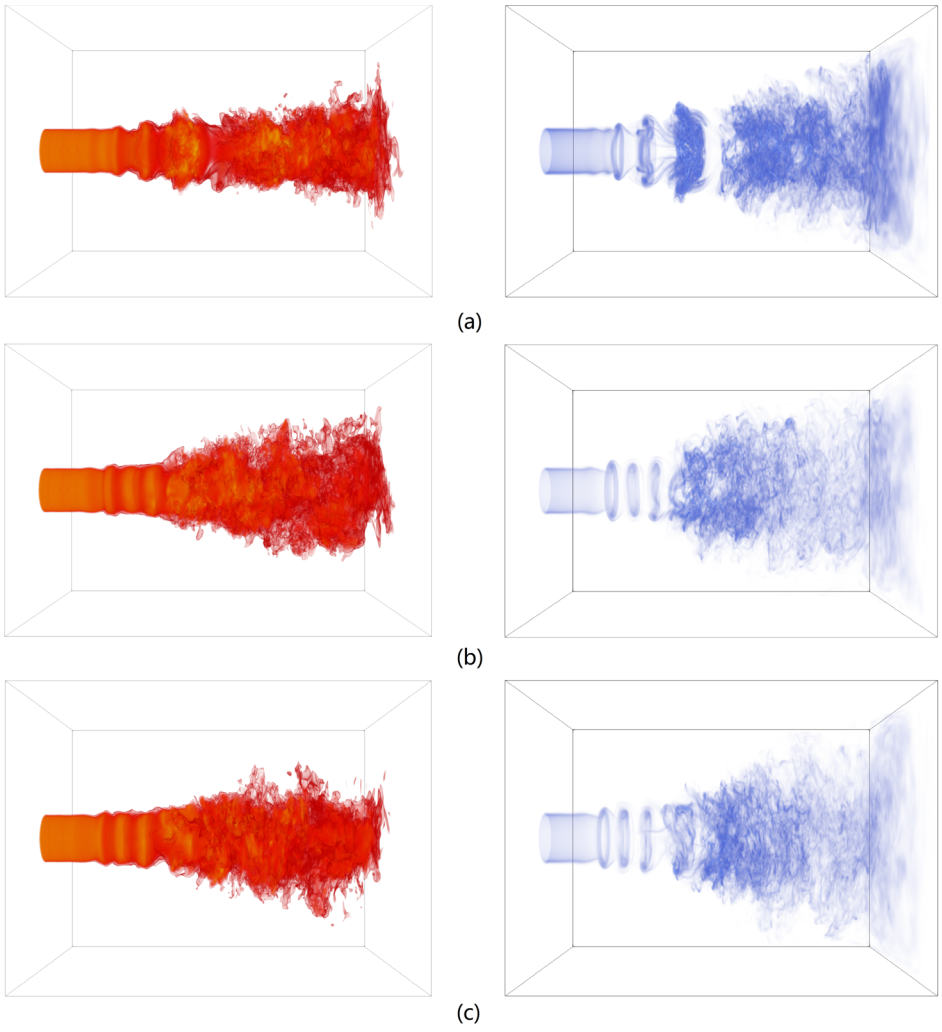

Fig. 6 Distribution of the data velocity field and the corresponding enstrophy in different time steps. **a** the start time step of the combustion simlulation. **b** the middle time step. **c** the end time step

- Compared to low enstrophy components, higher enstrophy components are more scattered and they will not last for a long time.
- The sizes of enstrophy components will increase first and then decrease. It reaches its peak at the middle time of the combustion process.

Acknowledgements
The authors would like to thank the Computer Network Information Center, Chinese Academy of Sciences and University of Chinese Academy of Sciences.

Authors' contributions
The contribution of the authors to this work is equivalent. All authors read and approved the final manuscript.

Authors' information
Xiaoyang Han is currently pursuing Ph.D. degree in University of Chinese Academy of Sciences, Beijing, China. His research interests are scientific visualization and visualization in AI. Contact him at hanxiaoyang@cnic.cn.
Yifei An is currently pursuing M.S. degree in University of Chinese Academy of Sciences, Beijing, China. Her research interest is flow visualization. Contact her at anyifei@cnic.cn.
Guihua Shan is with Computer Network Information Center, Chinese Academy of Sciences, Beijing, China. Her research interests are scientific visualization and interactive visualization. Contact her at sgh@cnic.cn.
Jun Liu is with Computer Network Information Center, Chinese Academy of Sciences, Beijing, China. His research interests are scientific visualization and parallel computing. Contact him at liujun@sccas.cn.

Bo Yang is with Computer Network Information Center, Chinese Academy of Sciences, Beijing, China. His research interests are scientific visualization and in-situ visualization. Contact him at yangbo@cnic.cn.

Funding
This work is supported by the Basic Research of the National Numerical Wind Tunnel Project (NNW2019ZT6-B19).

Availability of data and materials
Not applicable.

Declarations

Competing interests
The authors declare that they have no competing interests.

Received: 28 June 2021 Accepted: 2 January 2022
Published online: 23 February 2022

References

1. Poinsot T, Veynante D (2005) Theoretical and numerical combustion. 2nd edn. RT Edwards Inc, Philadelphia
2. Cecere D, Ingenito A, Giacomazzi E, Romagnosi L, Bruno C (2011) Hydrogen/air supersonic combustion for future hypersonic vehicles. Int J Hydrog Energy 36(18):11969–11984
3. Hin A, Post FH (1993) Visualization of turbulent flow with particles. In: Bergeron D, Nielson G (eds). Proceedings of the 4th conference on visualization '93 (VIS '93). IEEE Computer Society, Washington. pp 46–53
4. Mynett AE, Sadarjoen IA, Hin AJS (1995) Turbulent flow visualization in computational and experimental hydraulics. In: Proceedings of the 6th conference on visualization '95 (VIS '95). IEEE Computer Society, Washington. p 388
5. Johnson GP, Calo VM, Gaither KP (2008) Interactive visualization and analysis of transitional flow. IEEE Trans Vis Comput Graph 14(6):1420–1427. https://doi.org/10.1109/TVCG.2008.146
6. Gaither KP, Childs H, Schulz KW, Harrison C, Barth W, Donzis D, Yeung PK (2012) Visual analytics for finding critical structures in massive time-varying turbulent-flow simulations. IEEE Comput Graph Appl 32(4):34–45
7. Fu Y, Yu C, Yan Z, Li X (2019) The effects of combustion on turbulent statistics in a supersonic turbulent jet. Adv Appl Math Mech 11(3):664–674
8. Luo K, Jin T, Lu S, Fan J (2013) DNS analysis of a three-dimensional supersonic turbulent lifted jet flame. Fuel 108(11):691–698
9. Papamoschou D, Roshko A (1988) The compressible turbulent shear layer: an experimental study. J Fluid Mech 197:453-477
10. Li HM, Li GX, Jiang YH, Li L, Li FS (2018) Flame stability and propagation characteristics for combustion in air for an equimolar mixture of hydrogen and carbon monoxide in turbulent conditions. Energy 157:76–86
11. Wacks DH, Chakraborty N, Klein M, Arias PG, Im HG (2016) Flow topologies in different regimes of premixed turbulent combustion: A direct numerical simulation analysis. Phys Rev Fluids 1:083401. https://doi.org/10.1103/PhysRevFluids.1.083401
12. Rao S, Asano S, Saito T (2016) Comparative studies on supersonic free jets from nozzles of complex geometry. Appl Therm Eng 99:599-612
13. Rao S, Ikeda T, Asano S, Saito T (2017) Far-field hot-wire measurements on free jet from complex supersonic nozzles. Appl Therm Eng 118:670–681
14. Bogey C, Bailly C (2010) A study of the influence of the Reynolds number on jet self-similarity using large-eddy simulation. In: Armenio V, Geurts B, Fröhlich J (eds). Direct and large-eddy simulation VII. ERCOFTAC Series, vol 13. Springer, Dordrecht. https://doi.org/10.1007/978-90-481-3652-0_2
15. Zhou B, Li Q, He Y, Petersson P, Li Z, Aldén M, Bai XS (2015) Visualization of multi-regime turbulent combustion in swirl-stabilized lean premixed flames. Combust Flame 162(7):2954–2958
16. Slessor M, Zhuang M, Dimotakis PE (2000) Turbulent shear-layer mixing: growth-rate compressibility scaling. J Fluid Mech 414:35–45
17. Boersma BJ, Brethouwer G, Nieuwstadt F (1998) A numerical investigation on the effect of the inflow conditions on the self-similar region of a round jet. Phys Fluids 10(4):899–909
18. McLoughlin T, Laramee RS, Peikert R, Post FH, Chen M (2010) Over two decades of integration-based, geometric flow visualization. Comput Graph Forum 29(6):1807–1829
19. Han J, Wang C (2020) TSR-TVD: Temporal super-resolution for time-varying data analysis and visualization. IEEE Trans Vis Comput Graph 26:205–215
20. Guo L, Ye S, Han J, Zheng H, Gao H, Chen D, Wang J-X, Wang C (2020) SSR-VFD: Spatial super-resolution for vector field data analysis and visualization. 2020 IEEE Pacific Visualization Symposium (PacificVis), Tianjin. https://doi.org/10.1109/PacificVis48177.2020.8737
21. Chaudhuri A, Lee TY, Shen HW, Wenger R (2014) Exploring flow fields using space-filling analysis of streamlines. IEEE Trans Vis Comput Graph 20(10):1392–1404
22. Lu K, Chaudhuri A, Lee TY, Shen HW, Wong PC (2013) Exploring vector fields with distribution-based streamline analysis. 2013 IEEE Pacific Visualization Symposium, Sydney, 27 February - 1 March 2013
23. He W, Wang J, Guo H, Wang K-C, Shen H-W, Raj M, Nashed YSG, Peterka T (2020) InSituNet: Deep image synthesis for parameter space exploration of ensemble simulations. IEEE Trans Vis Comput Graph 1:23–33. https://doi.org/10.1109/tvcg.2019.2934312
24. Wilde T, Rössi C, Theisel H (2019) Recirculation surfaces for flow visualization. IEEE Trans Vis Comput Graph 25(1):946–955

25. Tao J, Wang C, Chawla NV, Shi L, Kim SH (2018) Semantic flow graph: A framework for discovering object relationships in flow fields. IEEE Trans Vis Comput Graph 24(12):3200–3213
26. Gordon S, McBride BJ (1976) Computer program for calculation of complex chemical equilibrium compositions, rocket performance, incident and reflected shocks, and Chapman-Jouguet detonations. NASA Tech Rep, NASA-SP-273
27. Lu S, Fan J, Luo K (2012) High-fidelity resolution of the characteristic structures of a supersonic hydrogen jet flame with heated co-flow air. Int J Hydrog Energy 37(4):3528–3539
28. Jin T, Luo K, Lu S, Fan J (2015) Direct numerical simulation of a supersonic lifted hydrogen jet flame: A priori study on combustion models. Acta Astronaut 109:52–64
29. Jin T, Luo K, Lu S, Fan J (2017) Analysis of conditional statistics of a supersonic jet flame in heated coflow via direct numerical simulation. Acta Astronaut 134:179–188
30. Silver D, Wang X (1998) Tracking scalar features in unstructured datasets. In: Proceedings Visualization '98, Research Triangle Park, NC, USA, 18-23 October 1998. pp 79–86
31. Matsuoka D, Araki F, Inoue Y, Sasaki H (2016) Event detection and visualization of ocean eddies based on SSH and velocity field. In: Paper presented at the European Geosciences Union General Assembly 2016, Vienna, Austria, 17-22 April 2016
32. Matsuoka D, Araki P, Sasakit H (2019) Event detection and visualization of ocean eddies simulated by ocean general circulation model. Int J Model Simul Sci Comput 10(3):1950018

Publisher's Note